Nonlinear Dyn (2014) 76:447–457
DOI 10.1007/s11071-013-1138-7

ORIGINAL PAPER

Decentralized CRONE control of nonsquare multivariable systems in path-tracking design

Najah Yousfi · Pierre Melchior · Patrick Lanusse · Nabil Derbel · Alain Oustaloup

Received: 28 February 2013 / Accepted: 26 October 2013 / Published online: 21 November 2013

Abstract In this paper, motion control and robust path tracking were extended to nonsquare MIMO (Multi-Input Multi-Output) systems having more outputs than inputs. A path-tracking design based on fractional prefilter approach has been developed and extended to control nonsquare MIMO systems. The nonsquare relative gain array (NRG) is used to assess the performance of nonsquare control systems based on steady-state information. The CRONE control approach developed for multivariable plants based on third-generation SISO CRONE methodology is combined with MIMO-QFT (Quantitative Feedback Theory) robust design methodology, taking into account the plant uncertainties. After the determination of CRONE controller, the parameter of prefilter has been optimized considering physical constraints of actuators and the tracking performance specifications. The proposed design is applied to an example.

Keywords CRONE control design · Fractional prefilters · Loop pairing · Multivariable process · Motion control · Nonsquare relative gain array (NRG) · Path tracking · Quantitative Feedback Theory (QFT)

N. Yousfi (✉) · N. Derbel
Control & Energy Management Laboratory (CEM), Sfax Engineering School, University of Sfax, BP W, 3038 Sfax, Tunisia
e-mail: yousfi.najah@yahoo.fr

P. Melchior · P. Lanusse · A. Oustaloup
UMR 5218 CNRS, Bordeaux Institute of Technology, University of Bordeaux, 351 cours de la Liberation, 33405 Talence cedex, France

1 Introduction

Various researches have been proposed in robust generation and path-tracking design. In order to reduce overshoots, a prefilter is used since it is easy to be implemented and adapted in industrial path-tracking designs. As presented by Davidson and Cole [2], the Davidson–Cole (DC) fractional-order prefilter is a useful prefilter whose main property is eliminating overshoots on the plant output. Using this type of prefilter, one can limit the resonance of the feedback control loop by a continuous variation of its two constitutive parameters, time constant τ and real order n.

Multivariable systems were the most interesting problem in industry because most of complex industrial processes are always Multi-Input Multi-Output (MIMO) systems [1, 3]. MIMO systems are more difficult to control due to the existence of interactions among input and output variables. The general problem in the QFT Two-Degree-Of-Freedom (TDOF) system is how to generate the feedback controller and the prefilter [4]. Specifications of most QFT problems are to put the responses of a closed-loop system into lower and upper bounds [4, 5]. QFT design techniques have been developed for highly uncertain linear time-invariant square MIMO systems [6–8]. The QFT approach can be combined with different controller types like the H_∞ design [9, 10] and the CRONE control approach [11].A MIMO-QFT robust synthesis approach has been used by Melchior [3], who applied it to a square MIMO system. The purpose of this work is extending [3, 11] to nonsquare MIMO systems.

The CRONE control-system design was initially developed by Oustaloup [12–14, 16, 19, 27, 28]. This methodology is based on fractional-order differentiation [15]. Fractional Calculus is a section of mathematics based on integrals and derivatives of real or complex order of an arbitrary function [17]. The CRONE control is a frequency domain design to provide robust controllers for perturbed plants using the common unity feedback configuration. For the nominal state of the plant, this approach consists in determining the open-loop transfer function that guarantees the desired specifications like accuracy, overshoot, and rapidity and that ensures the smallest variation of the stability degree for other states of the plant. The controller can be obtained from the ratio of the open-loop transfer function to the nominal plant transfer function taking into account the plant right half-plane zeros and poles. There are three CRONE control generations. Only the principle of the third generation is given in this paper.

As the fractional-order differentiation allows us to describe the open-loop transfer function with few parameters, the optimal transfer function to meet the specifications is easier to obtain. Furthermore, the CRONE control design takes into account the plant genuine structured uncertainty domains and is able to provide high-performance robust controllers. The CRONE control design has already been applied to multivariable systems [18, 20, 29, 32, 33].

In industry process, a square MIMO system is usually used. This type system has an equal number of inputs and outputs. Yet, when one of actuators is dysfunctional, then the studied system becomes having more outputs than inputs. This paper deals with the problem of a nonsquare MIMO system that has more outputs than inputs in path-tracking design.

A path-tracking design using the Davidson–Cole prefilter applied to square multivariable systems has been developed [21], so this paper is its extension to nonsquare MIMO systems. A combined CRONE control and MIMO-QFT structure have been used to verify the utility of using a fractional prefilter. The nonsquare relative gain array (NRG) [22] is a useful tool to analyze nonsquare multivariable systems. NRG is used to determine the interaction measurements. This approach can facilitate to square down the nonsquare multivariable systems.

Section 2 briefly presents the MIMO-QFT technique. A method to control structure selection of a nonsquare multivariable system is summarized in Sect. 3. Section 4 outlines the CRONE CSD methodology for multivariable plants. A fractional prefilter optimization is given in Sect. 5. Finally, an example is employed to illustrate the effectiveness of the proposed methodology to control a nonsquare multivariable system in Sect. 6.

2 MIMO-QFT structure

MIMO-QFT structure is given by Fig. 1.

$P = [p_{ij}]_{m\times m}$ is a given $m \times m$ plant transfer function matrix. The linear time-invariant P represents the uncertain plant to be controlled. P should be square and minimum-phase. The controller $G(s) = \mathrm{diag}[g_{ii}]$ reduces the uncertainty effects, and the prefilter matrix $F(s) = \mathrm{diag}[f_{ii}]$ leaves the response into the desired region.

The transfer matrix is presented by (see Fig. 1)

$$T = [I + PG]^{-1} PGF. \tag{1}$$

The plant transfer function matrix P must be nonsingular, so

$$\left[P^{-1} + G\right]T = GF. \tag{2}$$

The inverse matrix P^{-1} is decomposed to the form

$$P^{-1} = \Lambda + B, \tag{3}$$

where Λ is the diagonal part, and B is the anti-diagonal part of P^{-1}.

Equation (2) can be transformed to this form using (3):

$$T = [\Lambda + G]^{-1}[GF - BT]. \tag{4}$$

For a square MIMO system, a 2×2 system is equivalent to 4 subsystems (MISO structure), which is proved by Horowitz [7, 25] (see Fig. 2).

The elements of the matrix Q are expressed by

$$q_{ij} = \frac{\det(P)}{\mathrm{adj}(P_{ij})}. \tag{5}$$

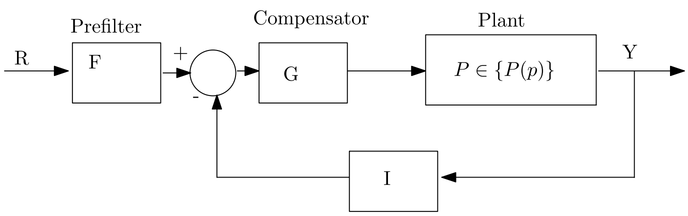

Fig. 1 Two-degrees-of-freedom control system: MIMO structure

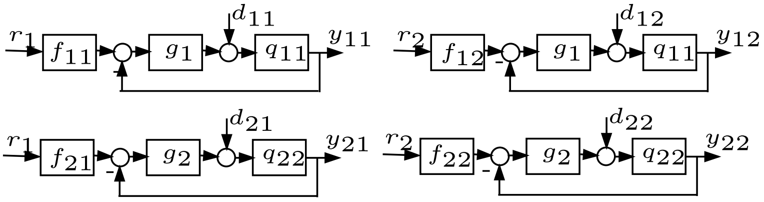

Fig. 2 Equivalent diagram for 2×2 MIMO system

The elements of the transfer matrix T have the following form:

$$t_{ij} = \omega_{ii}(v_{ij} + d_{ij}) = t_{r_{ij}} + t_{d_{ij}}, \tag{6}$$

where

$$\omega_{ii} = \frac{q_{ii}}{1 + g_i q_{ii}},$$

$$v_{ij} = g_i f_{ij}$$

and

$$d_{ij} = -\sum_{k \neq i}^{m} \left[\frac{t_{kj}}{q_{ik}}\right], \quad k = 1, 2, \ldots, m.$$

When d_{ij} appears as a "disturbance" [3], the MISO system design becomes a SISO-QFT design. The purpose of this methodology is to permit each loop track its desired input while minimizing the outputs caused by disturbance inputs [3].

To eliminate disturbances, there is a given limit to the responses $t_{d_{ij}}$ [26]. Let a small real positive function $\sigma_{ij}(\omega)$ be such that

$$\left|\frac{1}{1 + q_{ii}(j\omega) g_i(j\omega)}\right| \leq \left|\frac{\sigma_{ij}(\omega)}{-q_{ii}(j\omega)/q_{ij}(j\omega)}\right|, \quad i \neq j,\ j = 1, 2, \ldots, m. \tag{7}$$

3 Control structure for nonsquare multivariable systems

3.1 Nonsquare relative gain array (NRG)

Let P_1 an $m \times n$ transfer function matrix,

$$P_1(s) = \begin{pmatrix} p_{11} & p_{12} & \cdots & p_{1n} \\ \cdot & & & \cdot \\ \cdot & & & \cdot \\ p_{m1} & & \cdots & p_{mn} \end{pmatrix}, \tag{8}$$

where P_1 is an $m \times n$ process with $m \geq n$.

The nonsquare relative gain array is a way to measure interaction between inputs and outputs. The nonsquare relative gain array can be evaluated:

$$\Lambda^N(s) = P_1 \otimes \left(P_1^*\right)^T, \tag{9}$$

where the operator $\otimes$ is the Hadamard product, and P_1^* represents the Moore–Penrose pseudo-inverse transfer matrix of P_1.

$$\Lambda^N = \begin{pmatrix} \lambda_{11}^N & \lambda_{12}^N & \cdots & \lambda_{1n}^N \\ \cdot & & & \cdot \\ \cdot & & & \cdot \\ \lambda_{m1}^N & & \cdots & \lambda_{mn}^N \end{pmatrix}. \tag{10}$$

The sum of all elements in each row and each column is defined as

$$RS = \left[\sum_{j=1}^{n} \lambda_{1j}^N, \sum_{j=1}^{n} \lambda_{2j}^N, \ldots, \sum_{j=1}^{n} \lambda_{mj}^N\right]^T \tag{11}$$

$$= \left[rs(1), rs(2), \ldots, rs(m)\right]^T, \tag{12}$$

where $rs(i)$ is the sum of the ith row of the NRG, and

$$CS = \left[\sum_{i=1}^{m} \lambda_{i1}^{N}, \sum_{i=1}^{m} \lambda_{i2}^{N}, \ldots, \sum_{i=1}^{m} \lambda_{in}^{N} \right] \quad (13)$$

$$= \big[cs(1), cs(2), \ldots, cs(n)\big]. \quad (14)$$

Some properties of a nonsquare multivariable gain array (NRG) have been described by Chang [22].

- The sum of elements in each column of the NRG is equal to unity:

  $$cs(j) = 1 \quad \forall j$$

- The sum of elements in each row of the NRG is between zero and unity:

  $$0 \le rs(i) \le 1 \quad \forall i.$$

- The NRG is invariant under input scaling and variant under output scaling.
- Any permutation of rows and columns in the transfer function matrix P_1 results in the same permutation in the NRG.
- For an $m \times 1$ system, $P_1 = [p_{11}, p_{21}, \ldots, p_{m1}]^T$, so the NRG is described as follows:

  $$\Lambda^N = [\lambda_{11}, \lambda_{11}, \ldots, \lambda_{m1}]^T$$

  with

  $$\Lambda_{i1}^N = \frac{p_{i1}^2}{\sum_{k=1}^{m} p_{k1}^2}.$$

- The elements of the NRG approach infinity as the nonsquare system matrix P_1 becomes nearly singular.

3.2 Control structure selection

An approach to designing a control system for a nonsquare process has been developed by Chang [22]. This approach support the nonsquare system. Consider a nonsquare plant, P_1. It can be partitioned into a square subsystem P_s and a complementary (remaining) subsystem P_r. The control object is to minimize the sum of square error (SSE) of uncontrolled outputs when the square subsystem is under perfect control. The row sum of the NRG (Nonsquare Relative Gain array) provides some information in this regard.

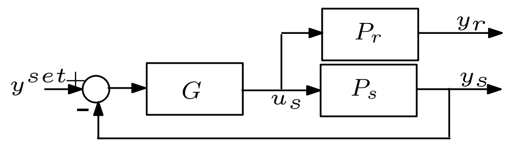

Fig. 3 Control structure for TDOF MIMO system

For an $m \times n$ process with $m > n$, if we choose n outputs for control, the system can be partitioned as shown in Fig. 3.

Then

$$\begin{bmatrix} y_s \\ - \\ y_r \end{bmatrix} = \begin{bmatrix} P_s \\ - \\ P_r \end{bmatrix} \times u = \begin{bmatrix} P_{11} & P_{12} & . & P_{1n} \\ . & . & . & . \\ P_{n1} & P_{n2} & . & P_{nn} \\ --- & --- & --- & --- \\ P_{m1} & P_{m2} & . & P_{mn} \end{bmatrix} \times u, \quad (15)$$

where y_s is an $n \times 1$ output vector for the controlled outputs, and y_r is an $(m-n) \times 1$ output vector for the remaining outputs. The aim is to minimize the Sum of Square Error (SSE) of the uncontrolled outputs for any variation in the controlled outputs.

The closed-loop square subsystem gains are given by

$$\tilde{u} = P_s^{-1} \tilde{y}_s^{\text{set}}. \quad (16)$$

For all outputs, the steady-state error is

$$\tilde{e} = \big(I_{m \times n} - P P_s^{-1}\big) \tilde{y}_s^{\text{set}}. \quad (17)$$

Choosing a particular square subsystem, P_s, the SSE is defined as

$$\text{SSE} = \sum_{i=1}^{n} \|\tilde{e}(i)\|_2^2 = \sum_{i=1}^{n} \|\big(I_{m \times n} - P P_s^{-1}\big) \tilde{y}_{s,i}^{\text{set}}\|_2^2. \quad (18)$$

The row sum of NRG provides an optimal solution to the problem for two special cases, namely, the case of $n = 1$ and the case of $m = n + 1$, and a suboptimal solution of other cases [22].

Case of $m = n + 1$ A square subsystem is chosen; the sum of square error is given by

$$\mathrm{SSE}(j) = \frac{rs(n+2-j)}{1 - rs(n+2-j)}, \tag{19}$$

where j means the sum of square error when the jth subset is chosen to form a square subsystem.

Since the value of the row sum is between zero and one, a small row sum gives a small SSE in the corresponding square subsystem. The small row sum of the NRG in the complementary system indicates a small SSE in the square subsystem. Then, the criterion for the selection of a square subsystem is to remove the controlled variable with the smallest row sum in the NRG. Other cases are well described by Chang [22].

4 3 G CRONE control

The CRONE control approach is a frequency-domain approach based on fractional-order differentiation. The objective of this method is how to design a controller which allows robustness of stability degree. There are three generations describing the control design approach. Because of various types of the plant frequency response uncertainties, in this paper we will deal with the third-generation CRONE control. The third-generation CRONE control can manage the robustness/performance tradeoff. For multivariable plant (MIMO), two methods have been developed multivariable [30] and multi-SISO approaches. The open-loop transfer functions β_{0_i} are used to satisfy some objectives:

- accuracy specifications at low frequencies,
- required nominal stability margins of the closed-loops,
- specifications on the control efforts at high frequencies.

The third generation of CRONE control system design (CSD) uses complex noninteger-order integration over an optimized frequency range $[\omega_A\ \omega_B]$. After a nonlinear optimization method, which permits the extraction of the independent parameters of each open-loop transfer function, frequency-domain system identification is used to approximate the fractional controller. All objectives cited above are satisfied by the open-loop transfer functions. For more detailed information about the design of a CRONE controller, we refer to [31].

The open-loop transfer function is based on

$$\beta_{0_i}(s) = C^{\mathrm{sign}(b)} \left(\frac{1 + s/\omega_h}{1 + s/\omega_l} \right)^{a} \times \left(Re_{/i} \left\{ \left(C_g \frac{1 + s/\omega_h}{1 + s/\omega_l} \right)^{ib} \right\} \right)^{-q\,\mathrm{sign}(b)} \tag{20}$$

with

$$C = ch\left[b \left(\arctan\left(\frac{\omega_{\mathrm{cg}}}{\omega_l} - \frac{\omega_{\mathrm{cg}}}{\omega_h} \right) \right) \right], \tag{21}$$

$$C_g = \left(\frac{1 + (\frac{\omega_{\mathrm{cg}}}{\omega_l})^2}{1 + (\frac{\omega_{\mathrm{cg}}}{\omega_h})^2} \right)^{1/2} \tag{22}$$

The corner frequencies are placed such that

$$\omega_l < \omega_A < \omega_{\mathrm{cg}} < \omega_B < \omega_h. \tag{23}$$

When the plant is stable and minimum phase, the open-loop transfer function that takes into account (20) is given by

$$\beta_{0_{ii}}(s) = \beta_{l_i}(s)\beta_{0_i}(s)\beta_{h_i}(s), \tag{24}$$

where

$$\beta_{l_i}(s) = C_{l_i} \left(\frac{\omega_{l_i}}{s} + 1 \right)^{n_{l_i}} \tag{25}$$

and

$$\beta_{h_i}(s) = \frac{C_{h_i}}{(\frac{s}{\omega_{h_i}} + 1)^{n_{h_i}}}. \tag{26}$$

The accuracy of each closed-loop is fixed by the order n_{l_i}, and the order n_{h_i} allows the elements of the controller to be proper.

5 Davidson–Cole prefilter optimization

The Davidson–Cole (DC) filter is described by the following transfer function:

$$F(s) = \frac{1}{(1 + \tau s)^{\eta}} = \frac{1}{(1 + \frac{s}{\omega})^{\eta}}, \tag{27}$$

where η is real and no longer restricted to being an integer.

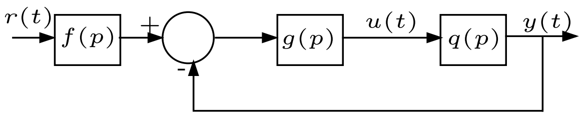

Fig. 4 Unity feedback control loop with prefilter

As an analog or the digital filter, it can be used to reduce overshoots in position control [33]. It is also very useful to limit the control effort sensitivity.

Considering Fig. 4, the reference to control the effort sensitivity transfer function S_{ref} between control u and input r is given by

$$S_{\text{ref}}(s) = \frac{F(s)G(s)}{1+G(s)Q(s)}. \tag{28}$$

In order to keep the control signal under its maximum value, the frequency-domain constraint is

$$\forall\omega > 0,\ \tau > 0, \quad \left|S_{\text{ref}}(j\omega)\right| \le \gamma, \tag{29}$$

where $\gamma = \frac{u_{\max}}{e_{\max}}$ with $u_{\max}$ the maximum static constraint value on the control signal and $e_{\max}$ a constant signal to apply on the prefilter input.

The desired range of the closed-loop transfer function is described by two bounds in frequency domain, which are detailed bellow:

$$\forall\omega > 0,\ \tau > 0, \quad \left|T_{\text{RL}}(j\omega)\right| \le \left|t_{r_{ii}}(j\omega)\right| \le \left|T_{\text{RU}}(j\omega)\right|. \tag{30}$$

These bounds become

$$\forall\omega > 0,\ \tau > 0, \quad \left|T_{\text{RL}}(j\omega)\right| \le \left|t_{r_{ii}}(j\omega)\right|_{\min}, \tag{31}$$

$$\left|t_{r_{ii}}(j\omega)\right|_{\max} \le \left|T_{\text{RU}}(j\omega)\right|, \tag{32}$$

with the closed-loop transfer function

$$t_{r_{ii}}(j\omega) = \frac{f_{ii}(j\omega)g_i(j\omega)q_{ii}(j\omega)}{1+g_i(j\omega)q_{ii}(j\omega)}. \tag{33}$$

By considering the integral gap criterion [3] we can obtain the optimized parameters of the Davidson–Cole filter. The integral gap analytic expression for step response is

$$I_e \le n\tau. \tag{34}$$

For $m \times m$ MIMO systems, the integral gap criterion is calculated as a MISO sub-system [3], so in the case of $F = \text{diag}[f_{ii}]$, Eq. (34) becomes

$$I_e \le n_1\tau_1 + n_2\tau_2 + \cdots + n_m\tau_m. \tag{35}$$

We can find the optimal parameters of (n, τ) using the optimization toolbox of *MATLAB*.

6 Application

Consider a 3×2 MIMO uncertain system. The transfer function matrix $P_1(s)$ is

$$P_1(s) = \begin{pmatrix} p_{11} & p_{12} \\ p_{21} & p_{22} \\ p_{31} & p_{32} \end{pmatrix}, \tag{36}$$

$$p_{ij}(s) = \frac{k_{ij}}{1+A_{ij}s}. \tag{37}$$

12 cases of plant are given in Table 1.

6.1 Pairing rules

From one to four plant conditions (Table 1), $P_1(0)$ is

$$P_1(0) = \begin{pmatrix} 1 & 0.5 \\ 1 & 2 \\ 0.7 & 5 \end{pmatrix}. \tag{38}$$

So, the NRG matrix Λ^N is described by

$$\Lambda^N = \begin{pmatrix} 0.7127 & -0.0645 \\ 0.4683 & -0.0554 \\ -0.1810 & 1.1199 \end{pmatrix}. \tag{39}$$

The sum of elements of each row of Λ^N is

$$RS = [0.6482 \quad 0.4129 \quad 0.9389]^T. \tag{40}$$

Observing the *RS* array (Eq. (40)), it is clear that the second output, which corresponds to the minimum value of *RS*, is the variable to be eliminated. Then, the rest of Λ^N becomes $\Lambda^{N'}$:

$$\Lambda^{N'} = \begin{pmatrix} [0.7127] & -0.0645 \\ -0.1810 & [1.1199] \end{pmatrix}. \tag{41}$$

According to the NRG matrix $\Lambda^{N'}$, the paired variables are $\{u_1/y_1, u_2/y_3\}$. The same technique is used for all other plants. From five to eight plant cases, the controller structure becomes $\{u_1/y_1, u_2/y_3\}$, and for the remaining plant cases, the variables are paired according to the form $\{u_1/y_1, u_2/y_2\}$.

A multiloop controller is now to be found to control the square subsystem.

6.2 Controller design

First, as proposed by the MIMO QFT methodology, the q_{ii} (5) elements of the equivalent matrix Q are computed. Then G_{11} and G_{22} of a decentralized controller G are designed by using the SISO CRONE control design tool.

The twelfth plant is considered as the nominal case. Some specification must be satisfied for all squared plants:

- For both outputs, zero steady-state error;
- Settling time as short as possible;
- Robustness according to disturbances and parametric variations;
- A first overshoot less than 5 %.

Considering these specifications, some elements of the open-loop transfer matrix can be initialized.

With all these specifications, the initial values for the parameters of the first fractional open-loop transfer function are [23, 24]

- $\omega_{cg} = 6.69$ rad/s,
- $\omega_l = 0.51$ rad/s ,
- $\omega_h = 7.32$ rad/s,
- $\|\beta_{0_1}(j\omega)\|_{\omega=\omega_r} = 0.51$ dB,
- $n_l = 1$,
- $n_h = 2$,

and, for the second,

- $\omega_{cg} = 15$ rad/s,
- $\omega_l = 3$ rad/s,
- $\omega_h = 75$ rad/s,
- $\|\beta_{0_2}(j\omega)\|_{\omega=\omega_r} = 2$ dB,
- $n_l = 1$,
- $n_h = 2$.

So, the optimization deals with the open-loop transfer function matrix $\beta_0(p)$:

$$\beta_0(s) = \begin{pmatrix} \beta_{0_1}(s) & 0 \\ 0 & \beta_{0_2}(s) \end{pmatrix}. \tag{42}$$

Taking into account all specifications, the optimal values for the various parameters of the open-loop transfer function matrix are the following:

- For the first loop, $C_{h1} \cdot C_{l1} = 8.1$, $a = 0.54$, $b = 0.24$, $q = 1$, and $C = 9.7$.
- For the second loop, $C_{h2} \cdot C_{l2} = 7.3$, $a = 1.2$, $b = -0.56$, $q = 1$, and $C = 5$.

Since

$$\beta_0(s) = \begin{pmatrix} q_{11_0}(s) & 0 \\ 0 & q_{22_0}(s) \end{pmatrix} G(s)$$

with

$$G(s) = \begin{pmatrix} G_{11}(s) & 0 \\ 0 & G_{22}(s) \end{pmatrix}, \tag{43}$$

the two diagonal elements of $G(s)$ are determined by the frequency domain:

$$G_{11}(s) = \frac{516.568(s + 1.38)(s + 0.476)}{s(s + 8.24)(s + 2.9)}, \tag{44}$$

$$G_{22}(s) = \frac{576.7369(s + 121)(s + 14.1)(s + 2.4)(s + 0.526)}{s(s + 95.8)(s + 32.7)(s + 12)(s + 3.58)}. \tag{45}$$

6.3 Prefilter synthesis

The tracking closed-loop transfer function is enforced to be under the following upper and lower bounds:

$$T_{\mathrm{RU}_{ii}}(s) = \frac{0.08s^2 + 3s + 25}{0.002s^3 + 1.015s^2 + 7.55s + 25}, \tag{46}$$

$$T_{\mathrm{RL}_{ii}}(s) = \frac{192}{s^4 + 19.5s^3 + 123s^2 + 272s + 192}. \tag{47}$$

The first step consists of selecting the maximum and minimum plants. The plants number one and eleven are respectively the minimum and maximum plants. Secondly, the ratio $\frac{u_{\max}}{e_{\max}} = 1$ is appointed. The optimized parameters are obtained by minimizing the integral gap criterion (Eq. (35)) with $m = 2$ while respecting the frequency bound inequality (Eq. (29)) and the performance specification (Eq. (30)):

$$\eta_1 = 1.8, \qquad \tau_1 = 0.2, \tag{48}$$

$$\eta_2 = 1.4069, \qquad \tau_2 = 0.202. \tag{49}$$

Using the CRONE Toolbox [23, 24, 31], the integer-order approximation of these prefilters is determined:

$$F(s) = \begin{pmatrix} F_{1\mathrm{DC}}(s) & 0 \\ 0 & F_{2\mathrm{DC}}(s) \end{pmatrix}, \tag{50}$$

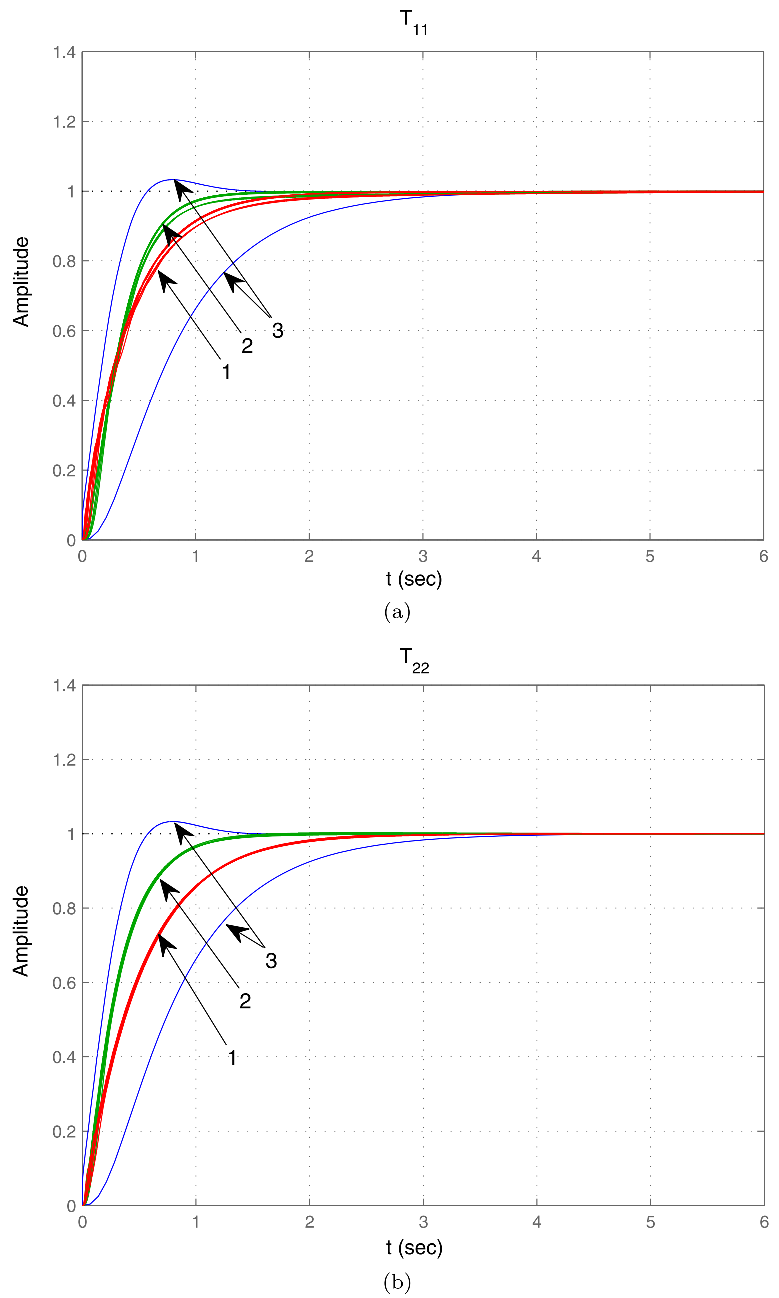

Fig. 5 (**a**, **b**) Closed-loop tracking response with classical (*1*) and fractional prefilters (*2*), tracking references (*3*)

where

$$F_{1DC}(s) = \frac{95.6862(s+497)(s+47)}{(s+889.1)(s+75.19)(s+7.196)(s+4.646)}, \tag{51}$$

$$F_{2DC}(s) = \frac{0.41778(s+889.5)(s+177.1)(s+44.29)}{(s+362.2)(s+118.9)(s+18.81)(s+3.6)}. \tag{52}$$

Under all twelve operating conditions, the time domain closed-loop tracking responses are illustrated using fractional- and integer-order prefilters F_{cl} in Fig. 6. The classical prefilter is described by the following expression:

$$F_{cl}(s) = \begin{pmatrix} F_{cl1}(s) & 0 \\ 0 & F_{cl2}(s) \end{pmatrix}, \tag{53}$$

Fig. 6 Disturbance step responses for all plant cases considering fractional prefilter

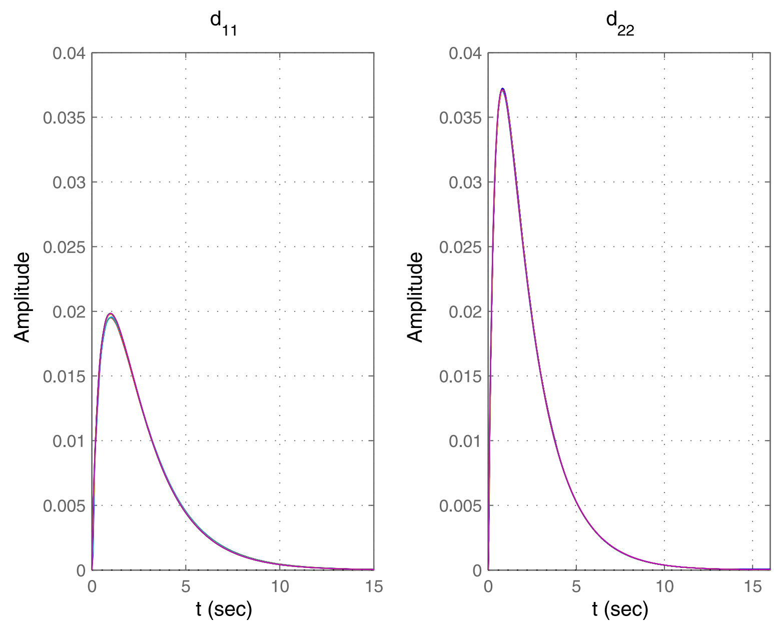

Table 1 Different conditions of uncertain MIMO systems

NO	k_{11}	k_{22}	k_{12}	k_{21}	k_{31}	k_{32}	A_{11}	A_{22}	A_{12}	A_{21}	A_{31}	A_{32}
1	1	2	0.5	1	0.7	5	2	2	4	4.5	2	2
2	1	2	0.5	1	0.7	5	0.5	1	1	3	3	2
3	1	2	0.5	1	0.7	5	0.2	0.4	0.5	2	1.5	2
4	1	2	0.5	1	0.7	5	0.7	0.8	0.3	1	2	2
5	4	5	1	2	3	6	1	2	2	4	4.5	2
6	4	5	1	2	3	6	0.5	1	1	3	3	2
7	4	5	1	2	3	6	0.2	0.4	0.5	2	1.5	3
8	4	5	1	2	3	6	0.7	0.8	0.3	1	2	3
9	10	8	2	4	1	7	1	2	2	4	4.5	3
10	10	8	2	4	1	7	0.5	1	1	3	3	3
11	10	8	2	4	1	7	0.2	0.4	0.5	2	1.5	3
12	10	8	2	4	1	7	0.7	0.8	0.3	1	2	3

where

$$F_{\mathrm{cl}1}(s) = \frac{2.5}{s+2.5}, \qquad F_{\mathrm{cl}2}(s) = \frac{2}{s+2}.$$

From Fig. 5, the closed-loop tracking specifications are respected, and no overshoots happened. All plant cases are under upper and lower bounds. The comparison between the two types of prefilters shows the benefit of using fractional prefilters like settling time reduction.

It is seen from Fig. 6 that disturbances are attenuated, so the specification of disturbance rejection has been successfully proved.

7 Conclusion

Motion control by fractional prefilter was extended to nonsquare MIMO systems, which is based on the MIMO-QFT robust control design combined with the CRONE control methodology. In terms of control structure selection, the NRG method has been used. After selection of the square subsystem, the CRONE control methodology is used to find the robust controller. Both parameters of the fractional Davidson–Cole prefilter are optimized on the multiple SISO systems taking into account the tracking specifications. Validation of this method is applied on a 3×2 MIMO system example. Future works will concern the application of this study to a MIMO real system and to extend this method to a general MIMO system with time delay.

References

1. Ho Choi, H.: Adaptive controller design for uncertain fuzzy systems using variable structure control approach. Automatica **45**, 2646–2650 (2009)
2. Davidson, D.W., Cole, R.H.: Dielectric relaxation in glycerol, propylene glycol and *n*-propanol. J. Chem. Phys. **19**(12), 1484–1490 (1951)
3. Melchior, P., Inarn, C., Oustaloup, A.: Path tracking design by fractional prefilter extension to square MIMO systems. In: Proceedings of the ASME 2009 International Design Engineering Technical Conference and Computers and Information in Engineering Conference, August 30–September 2, California, USA (2009)
4. Mohammad, S., Alavi, M., Khaki Sedigh, A., Labibi, B.: Pre-filter design for tracking error specifications in MIMO-QFT. In: 44th IEEE Conference on Decision and Control, and the European Control Conference, December 12–15, Seville, Spain (2005)
5. Boje, E.: Non-diagonal controllers in MIMO quantitative feedback design. Int. J. Robust Nonlinear Control **12**(4), 303–320 (2002)
6. Zenghui, W., Zengqiang, C., Qinglin, S., Zhuzh, Y.: Multivariable decoupling predictive control based on QFT theory and application in CSTR chemical process. Chin. J. Chem. Eng. **14**(6), 765–769 (2006)
7. Horowitz, I.: Survey of quantitative feedback theory (QFT). Int. J. Robust Nonlinear Control **11**(10), 887–921 (2001)
8. Skogestad, S., Postlethwaite, I.: Multivariable Feedback Control, Analysis and Design. Wiley, New York (1996)
9. Sidi, M.: A combined QFT/H∞ design technique for TDOF uncertain feedback systems. In: Proceedings of the 7th Mediterranean Conference on Control and Automation (MED99), Haifa, Israel, 28–30 June (1999)
10. Yousfi, N., Melchior, P., Rekik, C., Derbel, N., Oustaloup, A.: Path tracking design by fractional prefilter using a combined QFT/H_∞ design for TDOF uncertain feedback systems. J. Appl. Nonlinear Dyn. **1**(3), 239–261 (2012)
11. Yousfi, N., Melchior, P., Rekik, C., Derbel, N., Oustaloup, A.: Design of non-diagonal controller using MIMO-QFT approach combined with CRONE control: application to square system. In: Proceedings of the 5th IFAC Workshop on Fractional Differentiation and Its Applications, Hohai University, Nanjing, China, May 14–17 (2012)
12. Oustaloup, A.: Fractional order sinusoidal oscillators: optimization and their use in highly linear F.M. modulation. IEEE Trans. Circuits Syst. **8**(10), 1007–1009 (1981)
13. Oustaloup, A.: The CRONE control. In: Proceedings of the European Control Conference (ECC'91), Grenoble, France, 2–5 July (1991)
14. Oustaloup, A.: La commande CRONE. Hermes Science Publications, Paris (1991)
15. Kempfle, S., Schafer, I., Beyer, H.: Fractional calculus via functional calculus: theory and applications. Nonlinear Dyn. **29**, 99–127 (2002)
16. Lanusse, P.: From first generation to third generation of CRONE control. PhD thesis, Bordeaux I University, France (1994)
17. Tenreiro Machado, J.A.: Analysis and design of fractional-order digital control systems. Syst. Anal. Model. Simul. **27**(2–3), 107–122 (1997)
18. Oustaloup, A., Mathieu, B.: The CRONE Control: From Scalar to Multivariable. Hermes Editions, Paris (1999)
19. Oustaloup, A., Sabatier, J., Lanusse, P., Malti, R., Melchior, P., Moreau, X., Moze, M.: An overview of the CRONE approach in system analysis, modeling and identification, observation and control. In: 17th IFAC World Congress, Seoul, République de Corée, 6–11 July (2008)
20. Lanusse, P., Nelson Gruel, D., Sabatier, J., Lasnier, R., Oustaloup, A.: Synthèse multivariable d'une commande CRONE décentralisée. In: Borne, P., Filip, F.G., Benrejeb, M., Popescu, D. (eds.) Automatique Avancée et Informatique Appliquée, pp. 159–166. Editura Academiei Române, Bucuresti (2009). ISBN 9789732718063
21. Yousfi, N., Melchior, P., Rekik, C., Derbel, N., Oustaloup, A.: Path tracking design based on Davidson–Cole prefilter using a centralized CRONE controller applied to multivariable systems. Nonlinear Dyn. **71**, 701–712 (2013)
22. Chang, J.W., Yu, C.C.: The relative gain for non-square multivariable systems. Chem. Eng. Sci. **45**(5), 1309–1323 (1990)
23. www.ims-bordeaux.fr/CRONE/toolbox
24. Oustaloup, A., Melchior, P., Lanusse, P., Cois, O., Dancla, F.: In: The CRONE Toolbox for Matlab, IEEE International Symposium on Computer-Aided Control-System Design, Anchorage, USA, 25–27 September (2000)
25. Horowitz, I., Sidi, M.: Synthesis of feedback systems for prescribed time-domain tolerances. Int. J. Control **16**(2), 287–309 (1972)
26. Cheng, C.C., Liao, Y.K., Wang, T.S.: Quantitative feedback design of uncertain multivariable control system. Int. J. Control **65**(3), 537–553 (1996)
27. Oustaloup, A., Mathieu, B., Lanusse, P.: The CRONE control of resonant plants: application to a flexible transmission. Eur. J. Control **1**(2), 113–121 (1995)
28. Sabatier, J., Oustaloup, A., Garcia Iturricha, A., Lanusse, P.: CRONE control: principles and extension to time-variant plants with asymptotically constant coefficients. Nonlinear Dyn. **29**, 363–385 (2002)
29. Lanusse, P., Oustaloup, A., Mathieu, B.: Robust control of LTI square MIMO plants using two CRONE control design approaches. In: IFAC Symposium on Robust Control Design (ROCOND 2000), Prague, Czech Republic, 11–13 September (2000)

30. Yousfi, N., Melchior, P., Rekik, C., Derbel, N., Oustaloup, A.: Design of centralized CRONE controller combined with MIMO-QFT approach applied to non square multivariable systems. Int. J. Comput. Appl. **45**(16), 6–14 (2012)
31. CRONE research group, CRONE control design module user's guide. Version **4.0** (2010)
32. Nelson Gruel, D., Lanusse, P., Oustaloup, A.: Decentralised CRONE control of $m \times n$ multivariable system with time-delay. In: New Trends in Nanotechnology and Fractional Calculus Applications. Springer, Berlin (2009)
33. Nelson Gruel, D., Lanusse, P., Oustaloup, A.: Robust control design for multivariable plants with time-delays. Chem. Eng. J. **146**, 414–427 (2009)